Crystallization Behaviors of Poly(3-hydroxybutyrate) and Poly(L-lactic acid) in Their Immiscible and Miscible Blends

Jianming Zhang,[†] Harumi Sato,[†] Tsuyoshi Furukawa,[†] Hideto Tsuji,[‡] Isao Noda,[§] and Yukihiro Ozaki*,[†]

Department of Chemistry, School of Science and Technology, and Research Center for Environment Friendly Polymers, Kwansei-Gakuin University, Gakuen, Sanda 669-1337, Japan, Department of Ecological Engineering, Faculty of Engineering, Toyohashi University of Technology, Tempaku-cho, Toyohashi, Aichi 441-8580, Japan, and The Procter & Gamble Company, 8611 Beckett Road, West Chester, Ohio 45069

Received: August 14, 2006; In Final Form: September 19, 2006

By adjusting the molecular weight of the poly(L-lactic acid) (PLLA) component in poly(3-hydroxybutyrate) (PHB)/PLLA blends, we investigated the crystallization behaviors of the two components in their immiscible and miscible 50:50 blends by real time infrared (IR) spectroscopy. In the immiscible PHB/PLLA blend, the stepwise crystallization of PHB and PLLA was realized at different crystallization temperatures. PLLA crystallizes first at a higher temperature (120 °C). Its crystallization mechanism from the immiscible PHB/PLLA melt is not affected by the presence of the PHB component, while its crystallization rate is substantially depressed. Subsequently, in the presence of crystallized PLLA, the isothermal melt-crystallization of PHB takes place at a lower temperature (90 °C). It is interesting to find that there are two growth stages for PHB. At the early stage of the growth period, the Avrami exponent is 5.0, which is unusually high, while in the late stage, it is 2.5, which is very close to the reported value ($n \approx 2.5$) for the neat PHB system. In contrast to the stepwise crystallization of PHB and PLLA in the immiscible blends, the almost simultaneous crystallization of PHB and PLLA in the miscible 50:50 blend was observed at the same crystallization temperature (110 °C). Detailed dynamic analysis by IR spectroscopy has disclosed that, even in such apparently simultaneous crystallization, the crystallization of PLLA actually occurs faster than that of PHB. It has been found that, both in the immiscible and miscible blends, the crystallization dynamics of PHB are heavily affected by the presence of crystallized PLLA.

1. Introduction

Poly(L-lactic acid) (PLLA) ($-[CH(CH_3)COO]_n-$) is a biodegradable and biocompatible crystalline polymer that can be produced from renewable sources, such as corn.[1−5] Poly(3-hydroxybutyrate) (PHB) ($-[CH(CH_3)CH_2COO]_n-$), another type of environmentally degradable thermoplastic, is one of the most well-studied bacterial polyesters.[6−10] Both of them are representative biodegradable polyesters and have comparable or even sometimes superior thermal and mechanical properties to those of commercial polymers. Therefore, there is continuing interest in the investigations of their structure, physical properties, and applications.[11−18]

It is noteworthy that both PLLA and PHB have poor processing properties and are brittle at room temperature.[19,20] Thus, several modifications have been proposed to improve their processing and mechanical properties, such as copolymerization with other 3-hydroxyalkanoates and blending,[21−27] in which blending is a much easier and faster way compared to copolymerization methods. For the PHB/PLLA blends, their miscibility, crystallization, and melting behavior have been reported.[24−26] According to these studies, PHB is miscible with low molecular weight PLLA ($M_w < 18000$) in the melt at 200 °C over the whole composition range, whereas the PHB blends with much high-molecular-weight PLLA ($M_w > 18000$) show biphasic separation. Two types of spherulites are formed on cooling from the PHB/PLLA melt, respectively, relating to the crystallization of PHB and PLLA. In some blends, spherulites of different types are interpenetrated when the growth fronts collided. Owen et al.[25] proposed that lamellae belonging to one type of spherulite continues to grow in the interlamellar regions of the other type of spherulite. Recently,[27] physical properties of polymer alloys comprising PLLA and PHB and its copolymers are investigated. It was found that when a small amount of ductile PHB (10 wt %) is blended with PLLA, a new type of polymer alloy with much improved properties is created. The toughness of PLLA is substantially increased without the reduction in the optical clarity of the blend. The synergy between the two materials, both produced from renewable resources, is attributed to the retarded crystallization of PHB finely dispersed within a PLLA matrix as discrete domains.

In the past decades, many investigations have addressed the crystallization and positional distribution in miscible blends containing a single crystallizable component, that is, a miscible crystalline/amorphous blend. Only recently, much attention has been paid to the microstructure and confined crystallization of crystalline/crystalline blends.[28−34] It is reported that the crystallization behavior of two crystalline components in the blends is dependent on the miscibility, inert physical properties (T_g, T_m, etc.), and crystallization conditions of the two components. However, we notice that the effect of miscibility on the polymer

* To whom all correspondence should be addressed. Fax: +81-79-565-9077. E-mail: ozaki@kwansei.ac.jp.
[†] Kwansei-Gakuin University.
[‡] Toyohashi University of Technology.
[§] The Procter and Gamble Company.

10.1021/jp065233c CCC: $33.50
Published on Web 11/11/2006

crystallization in the blends is usually derived from different blend systems. As mentioned above, the miscibility of PHB/PLLA blends is strongly dependent on the molecular weight of the PLLA component. Therefore, blends of PHB and PLLA are of special interest, as not only are both components crystalline but also their miscibility can be easily adjusted by changing the molecular weight of PLLA.

Fourier-transform infrared spectroscopy (FTIR) is sensitive to the conformational and local molecular environment of polymers.[35,36] Thus, it has been extensively used as a convenient and powerful tool for investigating the crystallization process of semicrystalline polymers.[35−40,43] However, to our knowledge, no such application has been performed on the complex crystallization behavior in crystalline/crystalline blends. It is found that the investigations on the crystalline/crystalline blends heavily rely on small-angle X-ray scattering (SAXS), wide-angle X-ray diffraction (WAXD), and morphology data, such as atomic force microscopy (AFM) and transmission electron microscopy (TEM). These tools are, indeed, very useful for characterizing the crystalline phase of a semicrystalline polymer. However, for studying the crystallization mechanism of a polymer from the amorphous state to the crystalline state, that is to disclose the single chain motion, conformation transition, and chain packing in the whole crystallization process, IR and Raman spectroscopy have some distinct advantages.

It is of note that both PHB and PLLA crystallize into α form from melt and their crystalline structures belong to the same space group of orthorhombic $P2_12_12_1$-D^4_2. Since their unit cell contains the two helical chains in an antiparallel orientation rather than a single chain, it is rational to expect that crystallization sensitive bands caused by crystal field splitting or intermolecular interaction should appear in their corresponding crystallization processes. Actually, the crystallization sensitive bands of PHB and PLLA were well identified in our previous studies.[39,43] Therefore, it is feasible to in situ monitor the crystallization processes of PHB and PLLA in their blend systems by means of IR spectroscopy, which may provide new insight into the crystallization behavior of crystalline/crystalline blend.

In the present research, the physical origin of the miscibility in PHB/PLLA blends was examined by the comparison of the IR spectra measured at the melt states. It was found that there are potential intermolecular interactions, both in the immiscible and miscible PHB/PLLA blends. By adjusting the molecular weight of the PLLA component in PHB/PLLA blends, the crystallization behaviors of the two components in their immiscible and miscible 50:50 blends were investigated by real time IR spectroscopy. The stepwise crystallization of PHB and PLLA in immiscible blends and their simultaneous crystallization in miscible blends from the melt were clearly observed. The crystallization dynamic and mechanism on the two cases were analyzed and discussed in detail.

2. Experimental Section

2.1. Material and Preparation Procedures. The synthesis and purification of PLLA (M_w = 150000 and 4300 g mol^{-1}, M_w/M_n = 1.8 and 1.3, respectively.) were performed according to procedures reported previously.[2] Bacterially synthesized PHB (M_w = 600000 g mol^{-1}) was obtained from the Procter & Gamble Company, Cincinnati, OH. The melting points (T_m's) of PHB, high M_w PLLA, and low M_w PLLA used in the present study are, respectively, 172, 176, and 123 °C.

Blends of PHB and PLLA were prepared by dissolving them together in hot chloroform. Immiscible and miscible 50:50 blend films for the IR measurements were cast on a KBr window from 1% (w/v) PHB/PLLA (M_w = 150000 g mol^{-1}) and PHB/PLLA (M_w = 4300 g mol^{-1}) chloroform solutions. After the majority of the solvent had been evaporated, the films were placed under vacuum at room temperature for 48 h to completely remove the residual solvent. The thickness of such prepared polymer film was ca. 10 μm.

SCHEME 1: Thermal Program Used in This Study To Measure the IR Spectra during the Isothermal Melt-Crystallization Process of PLLA and PHB in the PLLA/PHB 50:50 Blend

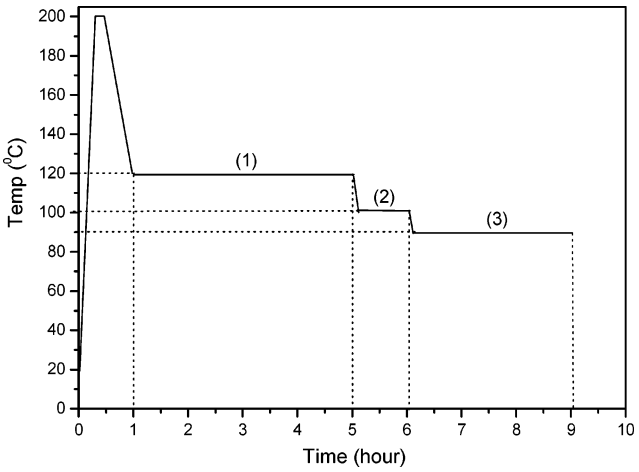

2.2. FTIR Spectroscopy. The thermal program shown in Scheme 1 was employed to perform the IR study of the stepwise isothermal melt-crystallization process of PHB and PLLA in the immiscible PHB/(high M_w) PLLA 50:50 blend. The KBr window with the sample was set on a homemade variable temperature cell, which was placed in the sample compartment of a Thermo Nicolet Magna 870 spectrometer equipped with an MCT detector. The sample was first heated at 10 °C/min up to 200 °C (about 25 °C higher than the melting point of PHB and PLLA) for 2 min to melt the polymer and erase the thermal history. It was then cooled at a rate of 5 °C /min to 120 °C for isothermal melt-crystallization. During the cooling period, we monitored structural changes in PHB/PLLA blends with real time IR measurements. From the real time IR spectra, we found that there was no crystallization occurring immediately after the sample was cooled to 120 °C, and that the crystallization rate of PLLA under this temperature was also suitable for our real time IR measurement. After finishing the crystallization of PLLA at 120 °C in 4 h, the sample was cooled to 100 °C and isothermally kept for 1 h, but no crystallization appeared. Subsequently, the sample was further cooled to 90 °C. The crystallization of PHB occurred and finished in 3 h.

For the IR study of the simultaneous crystallization process of PHB and (low M_w) PLLA in the miscible 50:50 blend, isothermal melt-crystallization temperature was chosen at 110 °C. It was found that 8 h is needed to finish the cocrystallization of PHB and PLLA under such conditions. IR spectra of the specimen were collected at a 2 cm^{-1} resolution with a 2 min interval during the annealing process. The spectra were obtained by coadding 16 scans.

3. Results and Discussion

3.1. Miscibility. As mentioned in the Introduction, from DSC and POM studies of the PHB/PLLA blend system,[24−26] it was well recognized that PHB is miscible with low molecular weight PLLA (M_w < 18000) in the melt at 200 °C over the whole

SCHEME 2: Chemical Structures of PHB and PLLA

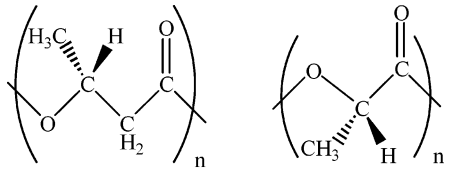

composition range, whereas the PHB blends with much higher molecular-weight PLLA (M_w > 18000) show biphasic separation. Such experimental conclusions are out of scope of the present study. Herein, we are interested in investigating the physical origin of this phenomenon. As shown in Scheme 2, the chemical structures of PLLA and PHB are very similar. Both of them belong to the biopolyesters, and the only difference between the repeat units of PLA and PHB lies just in the presence or absence of a single $-CH_2-$ group in the chain backbone. From the chemical structures, it seems that there is no specific interaction, especially the classical hydrogen-bonding interaction, between PHB and PLLA molecules. Usually, the effect of the molecular weight of the PLLA component on the miscibility of blends is interpreted on the basis of the Flory−Huggins theory. The interaction parameter χ_{12} between PHB and PLLA is directly related to the solubility parameters of the two components only if the potential interactions are ignored. In fact, this assumption has been well accepted by many researchers.[25,26] However, it is surprising to find out that there is no direct evidence reported from the spectral data on this fundamental assumption. In order to shed more light on the validity of this assumption, it is necessary to analyze the spectra of neat PHB, PLLA, and their immiscible and miscible blends in the melt state.

Figure 1a compares the IR spectra in the C═O stretching vibration region of PHB, high M_w PLLA, and their 50:50 blend at 200 °C. The corresponding second derivatives of these spectra, shown in Figure 1a, clearly reveal that there is only one component for neat PHB, but two components for PLLA. At 200 °C, both PHB and PLLA are in the melt states. It means only one component in the C═O stretching vibration region will be expected for their respective amorphous conformation in the homogeneous melts. For example, the single component, centered at 1740 cm^{-1} of the PHB in Figure 1a, is the expected one. However, it is surprising to find that two bands at 1776 and 1758 cm^{-1} are clearly resolved in the second derivative spectrum of neat PLLA. In our previous study on the melt-crystallization process of PLLA,[39] it was noted that the 1776 cm^{-1} band is not associated with an amorphous or a crystalline band. Therefore, this band might be a result from structure defects of PLLA. On the other hand, it is safe to assign the 1758 cm^{-1} band as the amorphous C═O stretching mode of PLLA, because its intensity decreases gradually with the crystallization. In the spectrum of 50:50 PHB/(high M_w) PLLA blend, three components could be resolved. Obviously, the component at 1776 cm^{-1} comes from that of PLLA, while the other two components (1750 and 1734 cm^{-1}) are different in the peak positions with the amorphous band of PHB at 1743 cm^{-1} and that of PLLA at 1758 cm^{-1}. It indicates that there is potential interaction even in the immiscible blend of PHB and PLLA.

Similarly, the comparison of the IR spectra of PHB, low M_w PLLA, and their 50:50 blend at 200 °C in the region 1800−1650 cm^{-1} is displayed in Figure 1b. In contrast to Figure 1a, besides the band at 1776 cm^{-1}, just one band is identified between the amorphous band of PHB and that of PLLA in the spectrum of 50:50 PHB/(low M_w) PLLA blend. Our spectral result is not in conflict with other groups' conclusion; that is, PHB is miscible with low M_w PLLA in the melt at 200 °C, whereas the PHB blends with high M_w PLLA show biphasic separation. However, it strongly suggests that there are potential specific interactions between PHB and PLLA molecules, because the obvious peak shifting of the C═O stretching band in the PHB/PLLA 50:50 blend spectra compared with that of the two individual components. Recently, we proposed that the weak $CH_3\cdots O{=}C$ interactions exist in the α crystal of PHB[9,10] and PLLA/PDLA stereocomplex.[40] Evidence for this type of hydrogen bonding has also been reported for matrix-isolated low-molecular-weight compounds.[41] Meanwhile, it should be noted that the peak shifting and half-width of C═O stretching band are also related to the intermolecular interaction induced by dipolar interactions.[42] It is not yet clear whether the $CH_3\cdots O{=}C$ interaction or dipole−dipole interaction is the main specific interaction between PHB and PLLA molecules. However, the results reported here clearly demonstrate that there are potential intermolecular interactions, both in the immiscible and miscible PHB/PLLA blends.

3.2. Crystallization Behavior in Immiscible PHB/PLLA Blend. The thermal program depicted in Scheme 1 was employed to study the crystallization behavior of the immiscible PHB/PLLA 50:50 blend. After being held at 200 °C for 2 min to erase any thermal history, the sample was cooled to 120 °C for isothermal crystallization. Figure 2 shows time-dependent IR spectra in the region 1850−820 cm^{-1} collected during the isothermal process of the immiscible PLLA/PHB blend at 120 °C for 240 min. Figure 3 shows the enlarged spectra and their corresponding difference spectra in the regions 1860−1720 cm^{-1} and 1500−1000 cm^{-1}, where the C═O stretching band and the CH_3, CH bending and C−O−C stretching bands appear, respectively. In the original IR spectra, many bands of PHB and PLLA are highly overlapped. Obviously, the difference spectra in Figure 3c,d more readily demonstrate the spectral changes during the isothermal crystallization process. In our previous studies,[39, 43] we reported the spectral changes during the melt crystallization process of PLLA and PHB. In the C═O stretching vibration region 1860−1720 cm^{-1}, PLLA and PHB, respectively, yield strong crystallization bands around 1759 and 1723 cm^{-1}. Thus, the two characteristic bands can be used to trace the crystallization process of PLLA and PHB, in the blends. In Figure 3a,c, only the temporal change of a strong crystallization band at 1759 cm^{-1} can be observed, and there is no change around the band at 1722 cm^{-1}. Moreover, as depicted in Figure 3d, it is noted that the spectral changes of the difference spectra in the region of 1500−1000 cm^{-1} are very similar to these derived from the melt-crystallization of pure PLLA reported in our previous study.[39] In this spectral region, the bands of PHB and PLLA are overlapped heavily. Fortunately, the amorphous band of PLLA at 1762 cm^{-1} is less overlapped. It will be taken for quantitative analysis together with the crystallization band around 1759 cm^{-1} later. Clearly, these spectral changes suggest that only the crystallization of PLLA occurs under the crystallization temperature. However, it should be noted that there are some subtle differences in the difference spectra of the C═O stretching vibration region (Figure 3d) compared to our previous report on the melt crystallization process of pure PLLA. In our previous report,[39] two split negative peaks appear at 1753 and 1745 cm^{-1} with the evolution of the crystallization of pure PLLA at 150 °C. Here, they are instead a small positive peak around 1749 cm^{-1} and negative

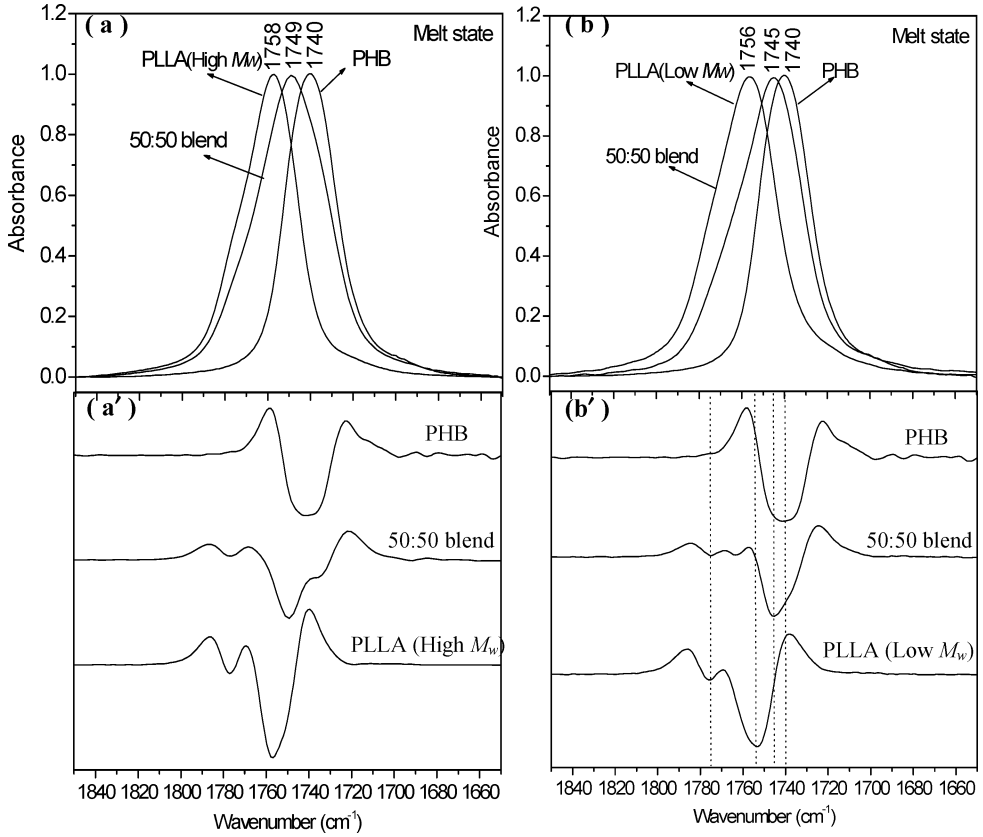

Figure 1. Comparsion of C═O stretching bands of PHB, PLLA, and their (a) immiscible and (b) miscible 50:50 blends at 200 °C. Normalized absorbance spectra are shown at the top panels (a, b), and their corresponding second derivative spectra are shown at the bottom panels (a′, b′).

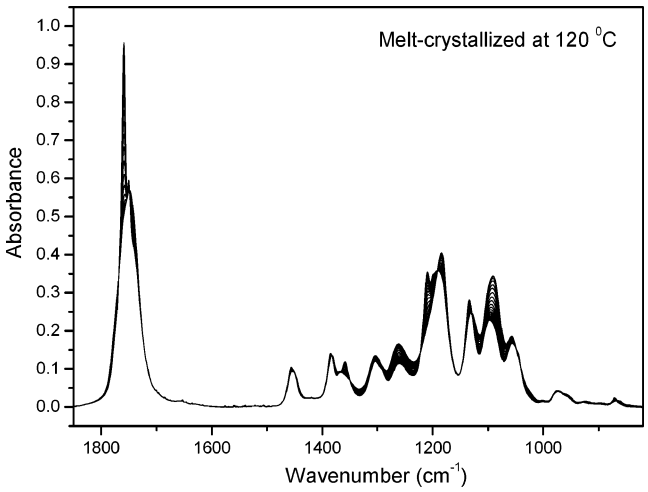

Figure 2. Time-dependent IR spectra in the region 1850−820 cm^{-1} collected during the isothermal process of the immiscible PLLA/PHB blend at 120 °C.

peak around 1744 cm^{-1}. Probably, the potential interactions between PHB and PLLA as mentioned above cause it.

To investigate the crystallization dynamic of PLLA from the PHB/PLLA blend melt, the normalized peak height of the crystalline sensitive band of PLLA at 1759 cm^{-1} calculated from the difference spectra (Figure 3c) is plotted in Figure 4a as a function of the crystallization time at 120 °C. The corresponding change in the amorphous band of PLLA at 1262 cm^{-1} is also depicted in Figure 4a. Obviously, they show the synchronous changes with time, which provide evidence that it is rational to characterize the crystallization process with the bands in the C═O stretching region. The crystallization curve suggests clearly that at least 240 min is needed to finish the crystallization of PLLA. Usually, in the neat PLLA system, the isothermal crystallization can be finished within 1 h in the temperature range 80−140 °C. Clearly, the crystallization rate of PLLA from the PLLA/PHB melt blend is depressed. In the immiscible blend of PLLA and PHB, the glass transition temperature (T_g) of PLLA is not affected by the presence of PHB melt. The T_g of polymer is generally related to the change of mobility of the crystallizable unit. Therefore, the mobility of the PLLA molecular unit should be the same as that in the neat homopolymer melt. The decrease of the crystallization growth rate of PLLA here should be caused by the dilution effect of PHB melt, which reduces the amount of PLLA chain segments toward the growing crystals.

When IR data in difference spectra are used, Avrami's equation[44] can be stated as below

$$\frac{A_t - A_\infty}{A_0 - A_\infty} = \exp(-kt^n) \tag{1}$$

where A_t is the peak intensity at the crystallization time t, A_∞ and A_0 are, respectively, the initial and final peak intensities during isothermal crystallization, k is the crystallization rate constant dependent on the nucleation and growth rates, t is the time of the crystallization, and n is Avrami exponent.[45] Equation 1 can also be expressed in the following form.

$$\ln\left[-\ln\left(\frac{A_t - A_\infty}{A_0 - A_\infty}\right)\right] = \ln k + n \ln t \tag{2}$$

Accordingly, the Avrami parameters n and k can be obtained from the slope and the intercept, respectively, by plotting the first term versus ln t. Figure 4b shows the Avrami plots of the crystallization dynamics of PLLA at 120 °C obtained by using

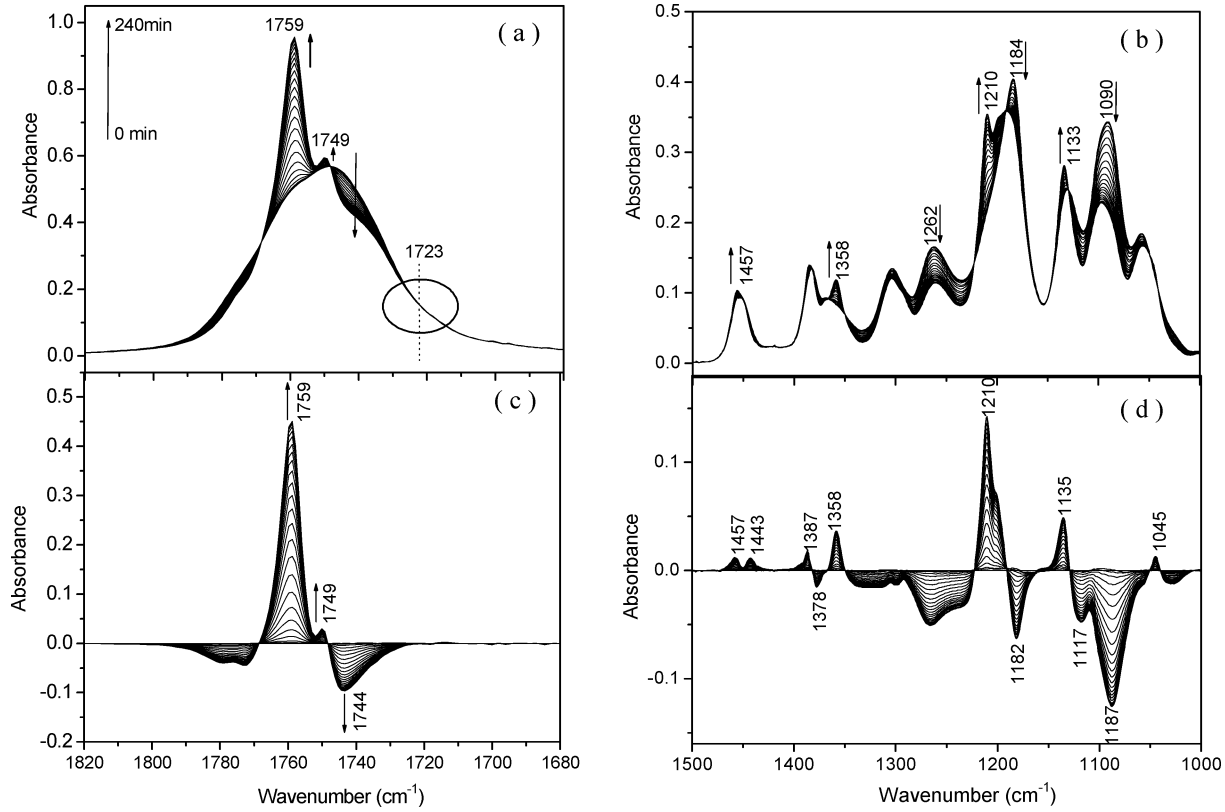

Figure 3. Temporal changes of the IR spectra in the regions (a) 1860−1720 and (b) 1500−1000 cm^{-1} during the isothermal process of immiscible PHB/PLLA blend at 120 °C. The spectra displayed were those measured with a 10 min interval. (c, d) Difference spectra calculated by subtracting the initial spectrum from the spectra shown in parts a and b, respectively.

the data in Figure 4a. The Avrami exponent is $n \approx 2$, which is similar to the value reported for the neat PLLA system.[39] An Avrami exponent is related to the nature of nucleation and the geometry of the growing crystals.[45] Therefore, the crystallization mechanism of PLLA from the immiscible PHB/PLLA melt is not affected by the PHB component. However, its crystallization rate is substantially depressed. Of particular note is that the Avrami plot shows an upward slope over the first few minutes, which corresponds to the induction period. One may wonder if there may be a systematic upward drift in the signal, due to the instrument instability. Actually, it was reported that there are conformation changes even in the induction period of polymer crystallization.[46,47] Meanwhile, with two-dimensional correlation analysis, we demonstrated that small but systematic spectral changes reflect the conformation rearrangement prior to the starting of crystallization rather than that caused by the instrument instability.[15,48] The fit of the initial portion of the data displays that the Avrami exponent is $n \approx 1$, which indicates the chain conformation rearrangement of PLLA in one low dimensional space due to the mixing of PLLA and PHB chains in the melt.

In order to observe the isothermal crystallization of PHB, the sample was cooled to 100 °C, at which the rapid crystallization growth of near PHB will occur.[49] However, as shown in Figure 5, there is no change in the crystallization sensitive C═O stretching vibration region after the sample was annealed at 100 °C for 1 h. Subsequently, it was further cooled to 90 °C for the isothermal crystallization. Figure 6a,b, respectively, display original IR spectral changes and difference spectra in the C═O stretching vibration region during the isothermal process. Obviously, there is almost no change for the crystalline band of PLLA at 1759 cm^{-1}, which indicates that only the crystallization of PHB takes place under such crystallization conditions. In Figure 6b, it is clearly seen that the crystalline band of PHB at 1723 cm^{-1} increases its intensity, while the amorphous band at 1743 cm^{-1} decreases. The profile of the spectral change in the difference spectra (Figure 6b) is the same as that in the melt crystallization process of neat PHB.[43]

Similarly, by calculating the normalized peak height of the crystalline band at 1723 cm^{-1} in the difference spectra (Figure 6b), the crystallization curve and corresponding Avrami plot of PHB can be derived (Figure 7). The S shape crystallization curve in Figure 7a indicates that, even in the presence of crystallized PLLA, PHB goes through the whole crystallization stages of a typical crystallizable polymer, which are induction, growth, and secondary crystallization periods. The crystallization of PHB was completed within 180 min. Usually, the Avrami plot is used to analyze the crystallization growth of a polymer by the linear fitting to obtain the crystallization dynamic parameters. However, in Figure 7b, it is interesting to find that there are two distinct growth stages. Therefore, two linear fittings are needed to describe the crystallization growth of PHB in the presence of crystallized PLLA. At the early stage of crystallization, the Avrami exponent is 5.0, which is unusually high and contrasts with the very low Avrami value ($n \approx 1$) of PLLA in the induction period as displayed in Figure 4b. Tashiro et al.[50] had observed the Avrami values of $n = 5$ for crystallization of syndiotactic polystyrene and suggested a three-dimensional conelike spherulite growth as a potential explanation for the large value of n. These phenomena have also been modeled with a distribution kinetics approach by Yang et al.[51,52] In the present study, it is not sure what is the practical growth mode for such a high Avrami value. However, it is noticed that PLLA crystallizes from the mixed melt of PHB and PLLA, while PHB crystallizes in a phase-separated system, where PLLA exists as a solid crystallization phase. The great difference in the Avrami values should reflect the different crystallization kinetics under the various confined environments. In the late

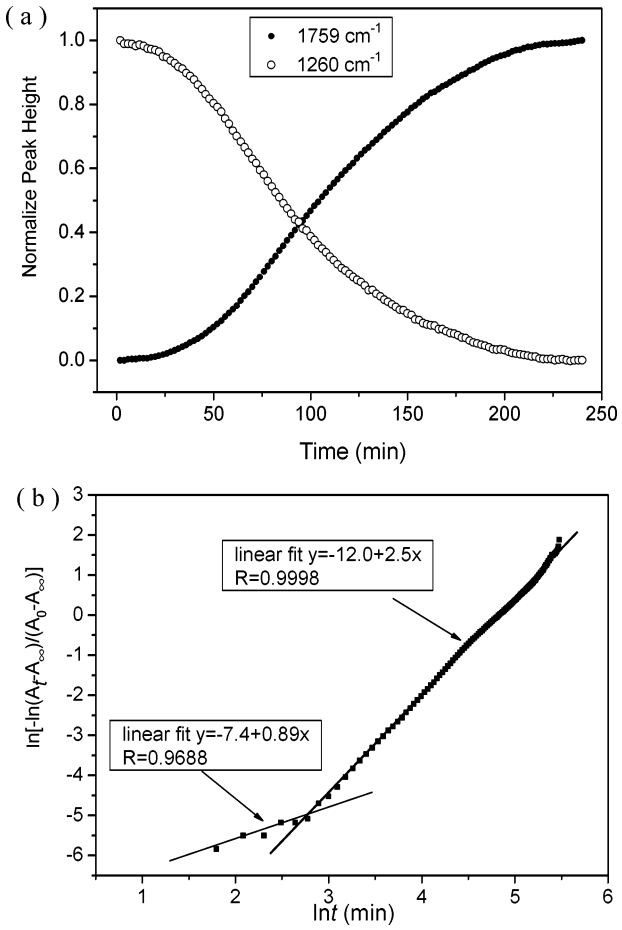

Figure 4. (a) Normalized peak heights of the crystalline sensitive band at 1759 cm^{-1} and the amorphous band at 1262 cm^{-1} of PLLA as a function of crystallization time at 120 °C. (b) Corresponding Avrami plot of the crystalline sensitive band at 1759 cm^{-1}.

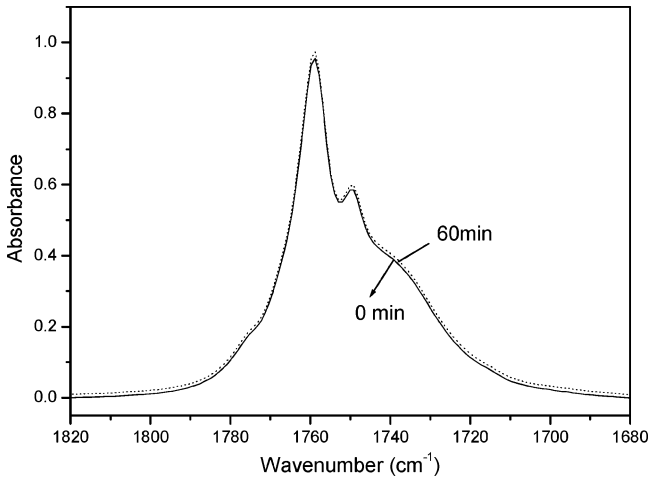

Figure 5. Comparison of the IR spectra of PLLA/PHB blend annealed at 100 °C for 0 and 60 min, respectively.

stage, the Avami value is 2.5, which is very close to the reported value ($n \approx 2.5$) for the neat PHB system.[43]

The above-mentioned isothermal crystallization conditions consist of the following two steps, namely, the isothermal crystallization of the PLLA phase at 120 °C from the melt, and the isothermal crystallization of the PHB at 90 °C from the liquid phase in the presence of previously crystallized PLLA. In the case of the crystallization of PLLA at 120 °C, the initial states of both PLLA and PHB are still in the amorphous melt. On the other hand, for the isothermal crystallization of PHB at 90 °C, the melt of PHB is dispersed in the crystallized solid of PLLA. For understanding such complex crystallization dynamics of PHB in the presence of PLLA crystals, the initial morphology of PHB after the completion of PLLA crystallization should be considered. There are two possibilities: (1) interlamellar segregation, that is, PHB melt exists in the areas between PLLA crystal lamellae; (2) interspherulitic segregation, with the PHB melt being segregated to the regions between the spherulites of PLLA. In any case, the confined crystallization of PHB in the presence of crystallized PLLA will be induced. Therefore, the complex crystallization dynamics of PHB in the presence of PLLA crystals may reflect the coexistence of different crystallization mechanism of PHB in such case.

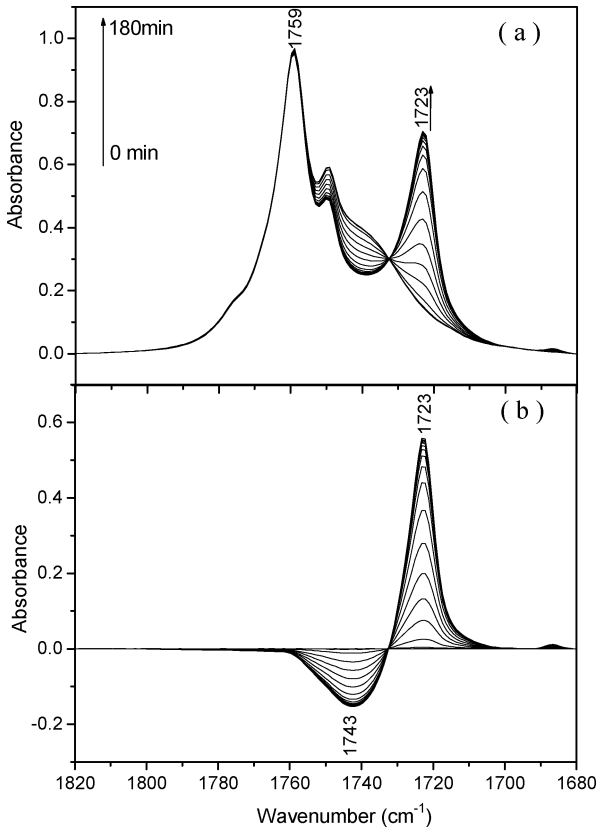

Figure 6. (a) Temporal changes of the IR spectrum in the region 1820−1680 cm^{-1} during the isothermal process of the immiscible PHB/PLLA blend at 90 °C. The spectra displayed were those measured with a 10 min interval. (b) Difference spectra calculated by subtracting the initial spectrum from the spectra shown in part a.

3.3. Crystallization Behavior in Miscible PHB/PLLA Blend. In contrast to the stepwise crystallization of PHB and PLLA in the immiscible blend, the simultaneous crystallization of PHB and PLLA can be observed in the miscible blend. Ikehara et al.[33] believed that when miscible crystalline/crystalline blends are crystallized from a homogeneous melt, the crystallization behavior largely depends on the difference in the melting point, T_m, of the two components. When the T_m difference is large, the component with higher T_m crystallizes first, and its spherulites usually fill the whole volume. The lower T_m component crystallizes at a lower temperature in spatially limited regions inside the spherulites of the other component. When the difference in T_m is small enough, both components have a high possibility to crystallize simultaneously. The T_m difference in most of the miscible crystalline/crystalline blends reported so far was about 100 °C. In these cases, the two components crystallize at different temperatures as described above. Here,

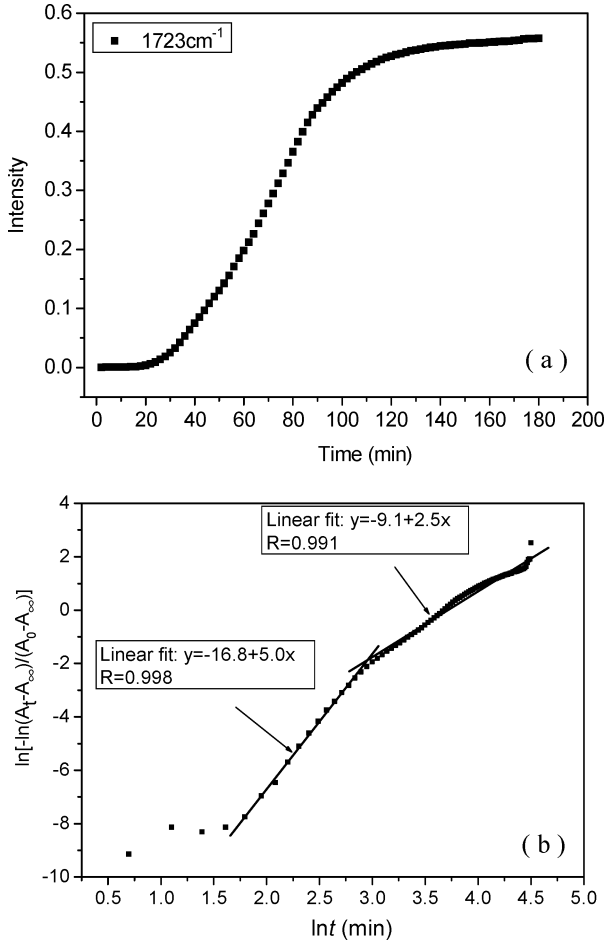

Figure 7. (a) The peak height of the crystalline sensitive band at 1723 cm^{-1} of PHB in the immiscible PHB/PLLA blend as a function of crystallization time at 90 °C. (b) Corresponding Avrami plot of part a.

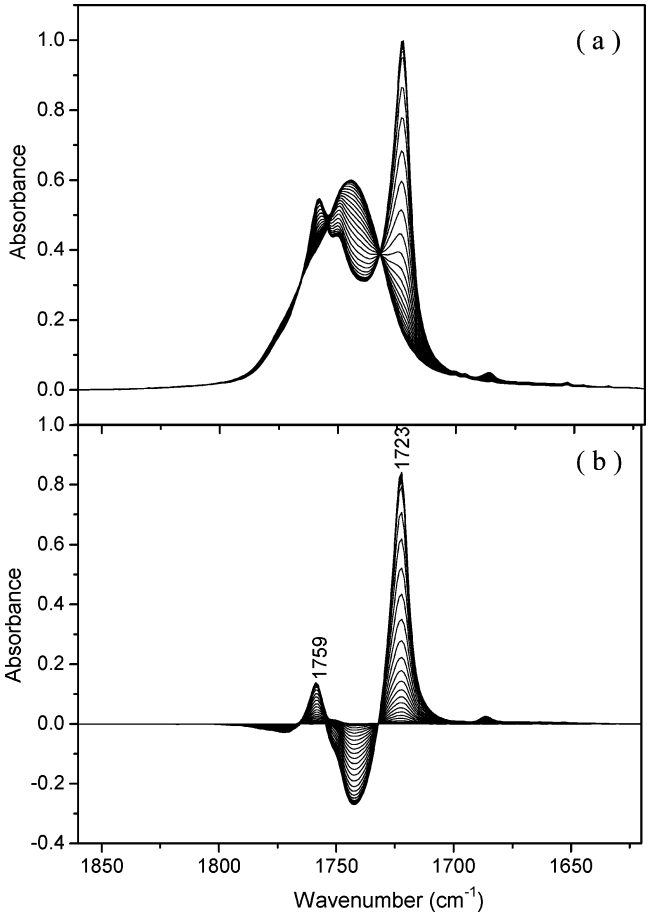

Figure 8. (a) Temporal changes of the IR spectrum in the region 1820−1680 cm^{-1} during the isothermal crystallization process of the miscible PHB/PLLA blend at 110 °C. The spectra displayed were those measured with a 10 min interval. (b) Difference spectra calculated by subtracting the initial spectrum from the spectra shown in part a.

the T_m difference between PHB and low M_w PLLA is about 47 °C. This leads to a possibility to realize the simultaneous crystallization as verified by Figure 8.

Figure 8a shows time-dependent IR spectra in the region 1850−820 cm^{-1} collected during the isothermal crystallization process of the miscible PLLA/PHB blend at 110 °C for 480 min. The comparison of the relative peak heights of the bands at 1759 and 1722 cm^{-1} in Figures 6a and 8a reveals that the final crystallinities of PLLA through such simultaneous crystallization are far lower than that of PHB. The result is in contrast to the case through the stepwise crystallization of PLLA and PHB in the immiscible blend as described above.

The increases in the characteristic crystallization bands of PLLA and PHB, respectively, at 1759 and 1723 cm^{-1} are clearly demonstrated in the corresponding difference spectra (Figure 8b). Figure 9a displays the crystallization curves of PHB and PLLA, which are calculated by the normalized peak intensity of the bands at 1723 and 1759 cm^{-1}. It can be seen from Figure 9a that the crystallization of PLLA takes place prior to that of PHB. The crystallization growth of PLLA starts at 50 min, while the PHB starts at 100 min. It is interesting to observe that there is a small dip when the intensity of the characteristic band of PLLA at 1759 cm^{-1} reaches its maximum value around 240 min. And at this time, the crystallization rate of PHB is the fastest. Since there is some overlap among the amorphous and crystalline C═O bands of PHB and PLLA, it is reasonable to assign the dip in the crystallization curve of PLLA to the fast depletion of PHB melt, when the crystallization rate of PHB is rapid around 240 min.

Figure 9b shows the corresponding Avrami plots of Figure 9a. The unusually low (0.9) and high (5.9) *n* values are, respectively, derived again for the initial and later stages of PHB crystallization. Polymers typically show Avrami exponents ranging from 2 to 4, reflecting growth in two or three dimensions from isolated nuclei.[45] The *n* value (3.4) of PLLA suggests a three-dimensional growth geometry and homogeneous nucleation. The *k* values in Figure 7b indicate that the crystallization growth rate of PHB is faster than that of PLLA, even though PLLA starts to crystallize earlier. Usually, the PLLA spherulites are often dendritic and grow much more slowly than the PHB spherulites. By morphology observation, Owen et al.[21] found that two types of spherulites are formed on cooling, relating to the crystallization of PHB and PLLA. In some blends, sperulites of opposite types interpenetrated when the growth fronts met. For the blend with 50% PHB, the crystallization of both types of spherulites could be observed simultaneously, with PHB spherulites generally growing faster than PLLA spherulites. When a PHB spherulite crystallization front reaches a PLLA spherulite, instead of growth being arrested, the PHB spherulite penetrates into the PLLA spherulite and the crystallization front becomes distorted. Therefore, the secondary crystallization process indicated in Figure 9b should be related to the interpenetrated crystallization process of PLLA and PHB.

Conclusion

By comparing the IR spectra of neat PHB and PLLA and their blends at the melt state, it is clearly demonstrated that there

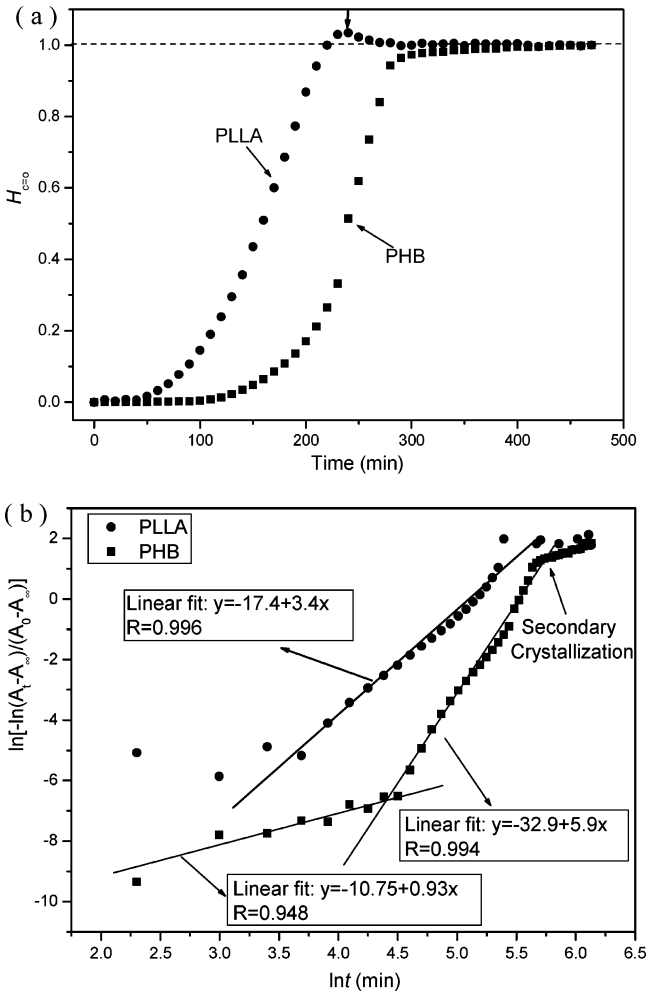

Figure 9. (a) Normalized peak heights of the crystalline sensitive bands of PLLA at 1759 cm^{-1} and PHB at 1722 cm^{-1} in the miscible PHB/PLLA blend as a function of crystallization time at 110 °C. (b) Corresponding Avrami plots of part a.

are potential interactions both in the immiscible and miscible PHB/PLLA blends. This result suggests that the previously reported interaction parameter χ_{12} between PHB and PLLA, which is just related to solubility parameters of the two components, may require some revision by considering the potential specific interactions.

The crystallization dynamics of PLLA and PHB in their immiscible and miscible 50:50 blends were investigated by real time IR spectroscopy. It is found that the two strong characteristic bands at 1759 and 1723 cm^{-1} are suitable for tracing the crystallization process of PLLA and PHB in the blends. In the immiscible PHB/PLLA blend, the stepwise crystallization of PHB and PLLA was realized at different crystallization temperatures. PLLA crystallizes first at a higher temperature. Its crystallization mechanism from the immiscible PHB/PLLA melt is not affected by the presence of the PHB component, while its crystallization rate is substantially depressed. Subsequently, in the presence of crystallized PLLA, the isothermal melt-crystallization of PHB takes place at a lower temperature. It is interesting to find that there are two growth stages for PHB. At the early stage of the growth period, the Avrami exponent is 5.0, which is unusually high, while in the late stage, it is 2.5, which is very close to the reported value ($n \approx 2.5$) for the neat PHB system. The complex crystallization dynamics of PHB in the presence of PLLA crystals may reflect the coexistence of different crystallization mechanisms of PHB under such a case. In contrast to the stepwise crystallization of PHB and PLLA in the immiscible blends, the almost simultaneous crystallization of PHB and PLLA in the miscible 50:50 blend occurs at the same crystallization temperature (110 °C). Detailed dynamic analysis by IR spectroscopy has revealed that, even in such apparent simultaneous crystallization, the crystallization of PLLA actually proceeds faster than that of PHB. However, the final crystallinities of PLLA are depressed largely by the simultaneous crystallization of PHB. Our research has clearly disclosed that the crystallization dynamics of PLLA and PHB are greatly affected by their miscibility in the blends.

Acknowledgment. Jianming Zhang thanks the Japan Society for the Promotion of Science (JSPS) for financial support. This work was partially supported by "Open Research Center" project for private universities: matching fund subsidy from MEXT (Ministry of Education, Culture, Sports, Science and Technology), 2001- 2008. This work was also supported by Kwansei-Gakuin University "Special Research" project, 2004-2008.

References and Notes

(1) Ikada, Y.; Tsuji, H. *Macromol. Rapid Commun.* **2000**, *21*, 117.
(2) Tsuji, H.; Ikada, Y. *Polymer* **1999**, *40*, 6699.
(3) Tsuji, H.; Ikada, Y. *Macromol. Chem. Phys.* **1996**, *197*, 3483.
(4) Urayama, H.; Kanamori, T.; Kimura, Y. *Macromol. Mater. Eng.* **2002**, *287*, 116.
(5) Dorgan, J. R. *Poly(lactic acid) Properties and Prospects of an Environmentally Benign Plastic*; The American Chemical Society: Washington, DC, 1999; pp 145−149.
(6) Doi, Y.; *Microbial Polyesters*; VCH Publishers: New York, 1990.
(7) Chiellini, E.; Solaro, R. *Recent Advances in Biodegradable Polymers and Plastics*; Wiley-VCH: Weinheim, 2003.
(8) Abe, H.; Doi, Y.; Aoki, H.; Akehata, T. *Macromolecules* **1998**, *31*, 1791.
(9) Sato, H.; Nakamura, M.; Padermshoke, A.; Yamaguchi, H.; Terauchi, H.; Ekgasit, S.; Noda, I.; Ozaki, Y. *Macromolecules* **2004**, *37*, 3763.
(10) Sato, H.; Murakami, R.; Padermshoke, A.; Hirose, F.; Senda, K.; Noda, I.; Ozaki, Y. *Macromolecules* **2004**, *37*, 7203−7213.
(11) Kobayashi, J.; Asahi, T.; Ichiki, M.; Okikawa, A.; Suzuki, H.; Watanabe, T.; Fukada, E.; Shikinami, Y. *J. Appl. Phys.* **1995**, *77*, 2957.
(12) Hoogsteen, W.; Postema, A. R.; Pennings, A. J.; ten Brinke, G. *Macromolecules* **1990**, *23*, 634.
(13) Cartier, L.; Okihara, T.; Ikada, Y.; Tsuji, H.; Puiggali, J.; Lotz, B. *Polymer* **2000**, *41*, 8909.
(14) Puiggali, J.; Ikada, Y.; Tsuji, H.; Cartier, L.; Okinara, T.; Lotz, B. *Polymer* **2000**, *41*, 8921.
(15) Zhang, J. M.; Duan, Y. X.; Sato, H.; Tsuji, H.; Noda, I.; Yan, S. K.; Ozaki, Y. *Macromolecules* **2005**, *38*, 8012−8021.
(16) Cornibert, J.; Marchessault, R. H. *J. Mol. Biol.* **1972**, *71*, 735
(17) Yokouchi, M.; Chatani, Y.; Tadokoro, H.; Teranishi, K.; Tani, H. *Polymer* **1973**, *14*, 267.
(18) Iwata, T.; Aoyagi, Y.; Fujita, M.; Yamane, H.; Doi, Y.; Suzuki, Y.; Takeuchi, A.; Uesugi, K. *Macromol. Rapid Comm.* **2004**, *25*, 1100.
(19) Zhang, L.; Goh, S. H.; Lee, S. Y. *Polymer* **1998**, *39*, 4841.
(20) Park, J. W.; Doi, Y.; Iwata, T. *Biomacromolecules* **2004**, *5*, 1557.
(21) Gassner, F.; Owen, A. J. *Polymer* **1994**, *35*, 2233.
(22) Abe, H.; Doi, Y.; Aoki, H.; Akehata, T. *Macromolecules* **1998**, *31*, 1791.
(23) Yoshie, N.; Saito, M.; Inoue, Y. *Macromolecules* **2001**, *34*, 8953.
(24) Koyama, N.; Doi, Y. *Polymer* **1997**, *38*, 1589.
(25) Owen, A. J.; Blumm, E. *Polymer* **1995**, *36*, 4077.
(26) Furukawa, T.; Sato, H.; Murakami, R; Zhang, J. M.; Duan, Y. X.; Noda, I.; Ochiai, S.; Ozaki, Y. *Macromolecules* **2005**, *38*, 6445.
(27) Noda, I.; Satkowski, M. M.; Dowrey, A. E.; Marcott, C. *Macromol. Biosci.* **2004**, *4*, 269.
(28) Chen, H. L.; Wang, S. F. *Polymer* **2000**, *41*, 5157.
(29) Qiu, Z. B.; Ikehara, T.; Nishi, T. *Macromolecules* **2002**, *35*, 8251.
(30) Qiu, Z. B.; Ikehara, T.; Nishi, T. *Polymer* **2003**, *44*, 2503.
(31) He, Y.; Zhu, B.; Kai, W.; Inoue, Y. *Macromolecules* **2004**, *37*, 3337.
(32) He, Y.; Zhu, B.; Kai, W.; Inoue, Y. *Macromolecules* **2004**, *37*, 8085.
(33) Ikehara, T.; Kimura, H.; Qiu, Z. B. *Macromolecules* **2005**, *38*, 5104.
(34) Herrera, D.; Zamora, J. C.; Bello, A.; Grimau, M.; Laredo, E.; Müller, A. J.; Lodge, T. P. *Macromolecules* **2005**, *38*, 5109.

(35) Chalmers, J. M.; Hannah, R. W.; Mayo, D. W. Spectra-structure correlations: Polymer spectra. In *Handbook of Vibrational Spectroscopy, Vol 4*; Chalmers, J. M., Griffiths, P. R., Eds.; John Wiley & Sons: Chichester, U.K., 2002; pp 1893−1918.
(36) Koenig, J. L. *Spectroscopy of Polymers*; The American Chemical Society: Washington, DC, 1992.
(37) Mallapragada, S. K.; Narasimhan, B. Infrared Spectroscopy in Analysis of Polymer Crystallinity. In *Encyclopedia of Analytical Chemistry*; Meyers, R. A., Eds.; John Wiley & Sons: Chichester, U.K., 2000; pp 7644−7658.
(38) Meaurio, E.; Zura, E.; Sarasua, J. R. *Macromolecules* **2005**, *38*, 1207.
(39) Zhang, J. M.; Tsuji, H.; Noda, I.; Ozaki, Y. *J. Phys. Chem. B.* **2004**, *108*, 11514.
(40) Zhang, J. M.; Sato, H.; Noda, I.; Ozaki, Y. *Macromolecules* **2005**, *38*, 4274.
(41) Matsuura, H.; Yoshida, H.; Hieda, M.; Yamanaka, S.; Harada, T.; Shin-ya, K.; Ohno, K. *J. Am. Chem. Soc.* **2003**, *125*, 13910.
(42) Painter, P. C.; Pehlert, J. G.; Hu, Y.; Coleman, M. M. *Macromolecules* **1999**, *32*, 2055.
(43) Zhang, J. M.; Sato, H.; Tsuji, H.; Noda, I.; Ozaki, Y. *Macromolecules* **2005**, *38*, 1822.
(44) Avrami, M. *J. Chem. Phys.* **1939**, *7*, 1103.
(45) Hay, J. N. *Br. Polym. J.* **1971**, *3*, 74.
(46) Imai, M.; Mori, K.; Mizukami, T.; Kaji, K.; Kanaya, T. *Polymer* **1992**, *33*, 4451.
(47) Strobl, G. R. *The Physics of Polymers*; Springer-Verlag: Berlin, 1996.
(48) Zhang, J. M.; Duan, Y. X.; Shen, D. Y.; Yan, S. K.; Noda, I.; Ozaki, Y. *Macromolecules* **2004**, *37*, 3292.
(49) Di Lorenzo, M. L. *Prog. Polym. Sci*. **2003**, 663.
(50) Yoshioka, A.; Tashiro, K. *Polymer* **2003**, *44*, 6681.
(51) Yang, J.; McCoy, B. J.; Madras, G. *J. Chem. Phys.* **2005**, *122*, 244905.
(52) Yang, J.; McCoy, B. J.; Madras, G. *J. Phys. Chem. B* **2006**, *110*, 15198.